Brazilian Journal of Chemical Engineering
https://doi.org/10.1007/s43153-023-00408-w

ORIGINAL PAPER

Fabrication of fluorescent PMMA-carbon nanodots optical films and their feasibility in improving solar cells efficiency using low-cost sustainable materials

Marco C. P. Soares[1] · Michele Cacioppo[2,6] · Francesco Amato[2,7] · Thiago D. Cabral[1] · Marcelo N. P. Carreño[3] · Inés Pereyra[3] · Carlos A. S. Ramos[3] · Manuel Cid[3] · Gilson S. Goveia[4] · José F. D. Chubaci[4] · Eric Fujiwara[1] · Julio R. Bartoli[1,5]

Received: 22 July 2023 / Revised: 12 September 2023 / Accepted: 22 September 2023

Abstract

Nitrogen-doped carbon nanodots synthesized from L-arginine and ethylenediamine (NCNDs); citric acid-derived carbon nanodots with carboxylic surface groups (α-CDs); and Silica-Cdots hybrids produced through coupling α-CDs to SiO_2 nanoparticles were used for the fabrication of fluorescent PMMA-CDs optical films. The nanoparticles occlusion allows the conversion of a broader UV bandwidth to the visible by enhancing PMMA's natural fluorescence. This UV-to-Visible conversion boost can enhance the efficiency of solar energy concentrators and generators and, as a proof-of-concept, photovoltaic cells were coated with NCNDs-doped PMMA films. Experiments show an 11.3% cell efficiency increase after film application, which can be further enhanced by optimizing film production and deployment, what shows the feasibility and potential of these low-cost environmentally friendly materials.

Marco C. P. Soares, Michele Cacioppo and Francesco Amato contributed equally to this work.

✉ Marco C. P. Soares
marcosoares.feq@gmail.com

✉ Michele Cacioppo
michelecacioppo@gmail.com

✉ Francesco Amato
amatofrancesco89@libero.it

✉ Julio R. Bartoli
bartoli@unicamp.br

[1] Laboratory of Photonic Materials and Devices, School of Mechanical Engineering, University of Campinas, Campinas, SP, Brazil

[2] Carbon Nanotechnology Group, Department of Chemical and Pharmaceutical Sciences, University of Trieste, Trieste, Italy

[3] Laboratory of Microelectronics, Polytechnic School, University of São Paulo (LME/EPUSP), São Paulo, SP, Brazil

[4] Institute of Physics, University of São Paulo, São Paulo, SP, Brazil

[5] School of Chemical Engineering, University of Campinas, Campinas, SP, Brazil

[6] Present Address: Department of Biological, Chemical and Pharmaceutical Sciences and Technologies (STEBICEF), University of Palermo, Viale Delle Scienze Ed. 17, 90128 Palermo, Italy

[7] Present Address: Department of Chemistry, University of Rome "La Sapienza", Rome, Italy

Published online: 19 October 2023

Graphical abstract

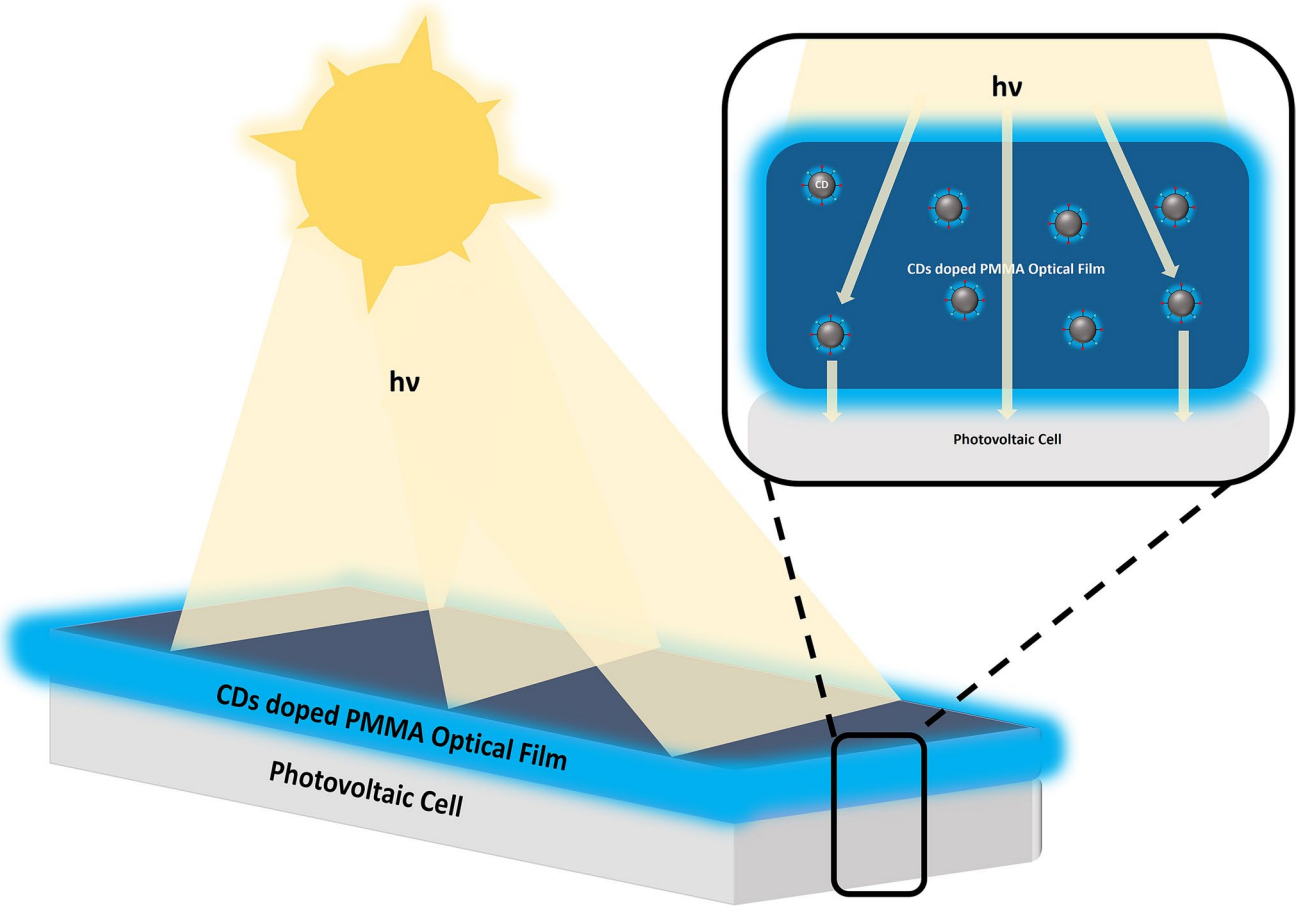

Keywords Carbon nanodots · Fluorescence · Photophysics · Photovoltaic devices · PMMA nanocomposites · Solar cells

Introduction

Carbon Nanodots (CDs) are fluorescent nanoparticles characterized by various surface functional groups and sizes below 10 nm (Wang and Hu 2014; Kang and Lee 2019). The conversion of organic precursors containing carboxylic acids (or nitrogen as doping element) results in the formation of CDs rich in carboxylic (or amine) surface groups with enhanced luminescence (Đorđević et al. 2022).

Beyond the low-cost, CDs are environmentally safe materials (Đorđević et al. 2022; Boakye-Yiadom et al. 2019) with good biological and biocompatibility properties, being excreted in urine (Wang and Hu 2014; Huang et al. 2013). The emission properties of CDs are altered by tuning their bandgaps¸ resulting a plethora of applications, such as in imaging and sensing, fabrication of optoelectronic devices, perovskite solar cells, graphene phototransistors, photocatalytic splitting of water, CO_2 reduction reactions, drug delivery and gene transfer (Đorđević et al. 2022; Wang and Lu 2022; Tuerhong et al. 2017). Energy applications also include the use of CDs to increase the efficiency of energy conversion in solar cells; to photosensitize or photocatalyze the conversion of solar energy into fuels; or to employ their fluorescence to prepare light emitting diodes (Đorđević et al. 2022). Their fluorescence properties also find use in light converters for photovoltaic cells and solar concentrators, and may replace dye sensitizers (Wang and Lu 2022; Tuerhong et al. 2017). Moreover, they can be combined with polymeric materials to obtain luminescent nanocomposites containing CDs (Perli et al. 2022; Amato et al. 2021, 2019; Gong et al. 2022, 2018; Li et al. 2023; Bouknaitir et al. 2019). Such polymer nanocomposites, in turns, may be produced through several techniques, including in-situ polymerization, cross-linking, solution blending, immersion precipitation and melt intercalation or exfoliation (Affonso Netto et al. 2022; Alexandre and Dubois 2000; Fischer 2003; Remanan et al. 2020; Bressanin et al. 2018; Prado and Bartoli 2018; Mazzucco et al. 2016). When nanoparticles dimensions are within the

molecular levels of polymer chains, these nanocomposites may exhibit enhanced physical properties.

For optical devices applications, the use of poly(methyl methacrylate), PMMA, is a particularly interesting polymer for designing transparent nanocomposite matrices (Affonso Netto et al. 2022; Bressanin et al. 2018; Prado and Bartoli 2018). PMMA is a highly transparent thermoplastic and an amorphous polymer in an intermediate position between commodities and engineering thermoplastics. It presents relative low cost, good mechanical strength and high optical transmittance (Ali et al. 2015; Corsaro et al. 2021). Thus, PMMA-CDs nanocomposites with fluorescence properties have potential applications in Light-Emitting Devices (LEDs) (Stepanidenko et al. 2021), Luminescent Solar Concentrators (LSCs) (Ma et al. 2019), Dye-Sensitized Solar Cells (DSCs) (Mohan et al. 2018) and Organic Solar Cells (OSCs) (Wang and Hu 2014; Bouknaitir et al. 2019; Maxim et al. 2020; Zhao et al. 2022; Lin et al. 2016; Kwon et al. 2013). In such cases, the polymer matrix is not only responsible for the device's mechanical support, but also for the dispersion of the nanodots and prevention of the solid-state quenching (Kwon et al. 2013).

In competition with CDs, organic dyes or inorganic quantum dots have been much more used as PMMA doping substances (Zhou et al. 2015; Waldron et al. 2017; Huang et al. 2023). However, the stability of organic dyes and toxicity of inorganic elements (CdTe, PbSe) (Moon et al. 2019; Albaladejo-Siguan et al. 2021; Manshian et al. 2017; Bottrill and Green 2011; Wu and Tang 2014) pose significant concerns. Furthermore, investigations on improving the luminescence quantum yield (QY) of CDs (ratio of emitted to absorbed photons) is currently a very active field of study in modern chemical science, through specialized synthesis routes to produce new doped carbon dots and to obtain unconventional luminescence profiles (Đorđević et al. 2019, 2020, 2022; Amato et al. 2019; Arcudi et al. 2016, 2017; Cacioppo et al. 2020; Cadranel et al. 2018; Ghosh et al. 2022; Xia et al. 2019; Yan et al. 2023). Recently, advanced approaches like the use of mechanochemistry, flow chemistry and laser synthesis in the liquid phase are widening the range of properties and applications of these promising nanomaterials. Besides, these novel synthesis methodologies present the advantage of being scalable. Finally, machine learning could be also applied to go beyond the trial-and-error approach commonly used to explore the chemistry of the CDs (Bartolomei et al. 2021).

Therefore, improvements in the energy conversion efficiency of solar cells can be achieved with LSCs or Luminescent Down Shifting (LDS) devices using low-cost and environmentally friendly fluorescent carbon dots (Gong et al. 2018; Li et al. 2017; Choi et al. 2017; Zhao 2019) instead of organic dyes or inorganic quantum dots. Considering these aspects, this work investigates the fabrication of PMMA optical films doped with fluorescent carbon nanodots. CDs exhibit a good solubility in polar solvents like methanol, whereas PMMA is very soluble in chloroform. As it was previously demonstrated that 2:1 (v/v) is the best ratio between chloroform and methanol to dissolve CDs chloroform (Amato et al. 2019; Soares et al. 2023), this proportion was applied to the solutions of PMMA to produce functionalized films by drop-casting. Three different kinds of CDs were synthesized and tested regarding the fluorescent emissions. Finally, solar cells were coated with these nanocomposite films for proof-of-concept experiments on increasing their energy conversion efficiency.

Materials and methods

Nitrogen-doped carbon nanodots synthesis

Blue-emitting nitrogen-doped carbon nanodots (NCNDs) from L-arginine (Fluorochem; ≥ 98%) and ethylenediamine (EDA, Sigma-Aldrich; ≥ 99.5%) are obtained through the bottom-up procedure previously described in literature (Arcudi et al. 2016).

Two organic precursors at 1:1 (mol/mol) ratio are mixed to ultrapure water (> 18 MΩ Milli-Q, Millipore): 87.0 mg of arginine are mixed to 33.0 µL EDA in 100.0 µL Milli-Q water and this solution is introduced into a CEM Discover-SP microwave oven with controlled conditions (240 °C, 26 bar and 200 W) for 180 s (reaction represented in Fig. 1a). The microwave treatment converts the transparent medium into a brown-colored solution (Fig. 1b), which is then diluted in water and filtered through a 0.1 µm microporous membrane for separating a deep yellow liquid (Fig. 1c). As shown in Fig. 1d, this filtered solution emits a strong blue fluorescence when irradiated with 365 nm ultraviolet (UV) light (Đorđević et al. 2019). Finally, the yellow solution is dialyzed against pure water through a dialysis membrane with molecular weight cut-off of 0.5–1 kDa (Spectrum Labs) for 2 days (water refreshed every 6 h) (Amato et al. 2019).

The dialyzed solution of NCNDs is lyophilized using a bench-top freeze-dryer (LaboGene ScanVac CoolSafe; − 49 °C; 72 h of vacuum). Each synthesis results in 23.0 mg of a brownish solid, so eleven batches are run to obtain 250 mg of NCNDs. It is demonstrated that this procedure is quite reproducible, and previous characterizations reveal that the obtained fluorescent NCNDs present relative quantum yield (QY) of 0.17 (Arcudi et al. 2016); narrow distribution of diameters (1.0–4.5 nm); and plenty of surface traps and functional groups that allow tuning the luminescent emissions. Besides, nitrogen doping has been reported to give excellent optical properties and usually blue-shifted fluorescence (Arcudi et al. 2016). The NCNDs fluorescence shows a broad emission peak at 356 nm when excited at 300 nm

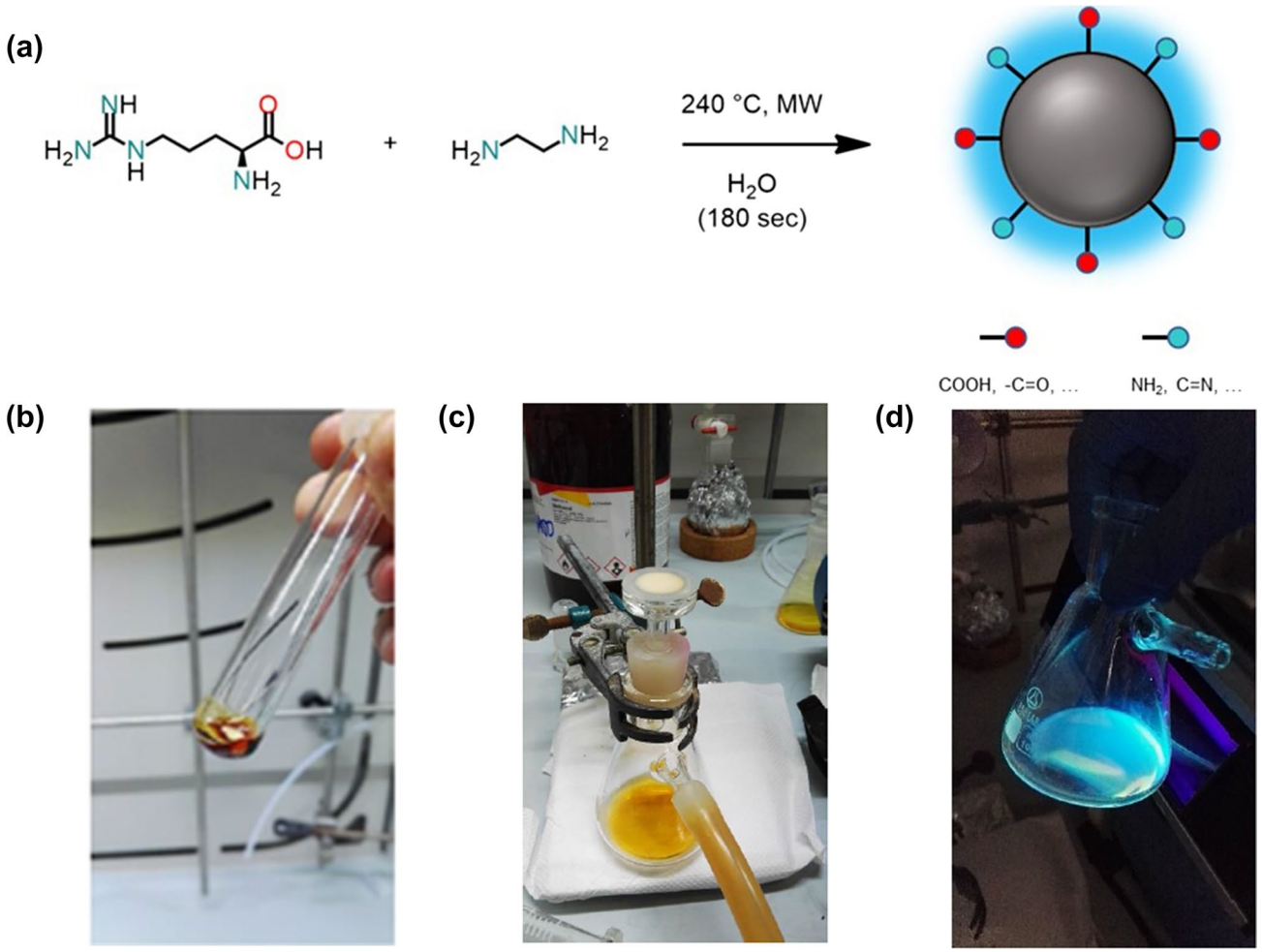

Fig. 1 **a** Scheme of formation of blue-emitting NCNDs; **b** brown-colored solution obtained after microwave-assisted synthesis; **c** yellow solution obtained after filtering; and **d** emission of blue fluorescence by the filtered solution when it is irradiated at 365 nm UV light (Amato et al. 2019)

and a bathochromic shift from 356 to 474 nm as the excitation changes from 300 to 420 nm (Đorđević et al. 2019; Arcudi et al. 2017).

It is worth noticing that these NCNDs were previously submitted to the Photoelectron Spectroscopy (XPS) characterization by Arcudi et al. to provide their chemical composition (part of the characterization protocol applied to each CD synthesized in the laboratories of the Carbon Nanotechnology Group) (Arcudi et al. 2016). It was reported the detection of C (68.0%), N (16.1%) and O (15.9%) with peaks at 286.8 eV (C1s), 400.33 eV (N1s) and 532.34 eV (O1s), respectively. The chemical moieties of C and N were further analyzed by deconvoluting their spectrum. C1s was deconvoluted into five surface components: sp^2 (C=C) at 274.5 eV; sp^3 (C–C and C–H) at 285.5 eV; C–O/C–N at 286.2 eV; C=O/C=N at 288.3 eV; as well as COOH at 290.5 eV. In turn, N1s spectrum was deconvoluted into four peaks centered at 398.3, 399.6, 400.5, and 401.9 eV, corresponding to C=N, NH_2, C–N–C and N–C_3, respectively. The presence of primary amino groups was confirmed by a positive Kaiser test (Arcudi et al. 2016).

α-CDs and Silica-Cdots hybrids production

Citric acid-derived carbon nanodots (α-CDs) and the nanocomposites formed by combining them with SiO_2 nanoparticles (Silica-Cdots) are used as produced and characterized in a previous (open access) report (Amato et al. 2021).

Briefly, α-CDs with sizes from 4 to 10 nm (mostly around 6 nm) are synthetized from the thermolysis of citric acid (200 g, Fluka, 99.5%) in a muffle furnace under air atmosphere at 180 °C for 40 h. In turns, commercial fumed silica nanoparticles (206 mg Aerosil 300, primary particle size ca. 7 nm, Evonik) are dispersed in ethanol (5 mL) and treated with 3-aminopropyltriethoxysilane (APTES, 5 mL). This dispersion is stirred overnight at room temperature (r.t.) before being purified by centrifugation; dispersed in ethanol

(three times); and lyophilized for obtaining amino-functionalized silica nanoparticles (a-SiO_2).

Finally, a-SiO_2 (50 mg) is mixed to the α-CDs (223 mg) dispersed in dry dimethylformamide (DMF, 10 mL) in the presence of 1-ethyl-3-(3-dimethylaminopropyl) carbodiimide hydrochloride (200 mg, EDC•HCl Alfa Aesar) and N-hydroxysuccinimide (120 mg NHS, Sigma Aldrich). This mixture is stirred at 70 °C for 2 days under inert atmosphere (Ar), and DMF is removed through azeotropic distillation with toluene. Milli-Q water is added, and the system is purified by centrifugation (two cycles of 20 min at 3000 rpm) for obtaining Silica-Cdots nanohybrids with sizes on the order of 50 nm, nitrogen and oxygenated surface groups, and excitation-dependent fluorescence. The maximum intensity is observed for the 360 nm-excitation (emission at 465 nm), and the emission shifts from 465 to 513 nm (green) as the excitation changes from 360 to 430 nm. FT-IR, TGA, XPS, XRD analysis and Raman spectra of the α-CDs and Silica-Cdots nanoparticles are readily available in the Supporting Information document accompanying the reference (Amato et al. 2021).

Preparation of doped-PMMA optical films

The synthesized carbon nanodots are used to prepare nanocomposites with PMMA by solution blending: PMMA pellets are dissolved in chloroform, whereas previously lyophilized nanodots are dispersed in a solution of methanol and chloroform. The solutions are mixed, and thin films of nanocomposites are finally prepared by drop-casting on a glass substrate (Petri dishes).

PMMA pellets (Plexiglas V0 52, Arkema) are dried in an oven for 4 h at 80 °C and subsequently cooled to room temperature in a vacuum chamber with drier agent. For the preparation of a PMMA optical film by casting, a ratio of 21.5:1 (mL/g) of chloroform (Sigma-Aldrich) to PMMA is used, and the system is left under magnetic stirring for 2 h at room temperature, followed by 20 s of ultrasound bath.

Lyophilized carbon nanodots are dispersed in a mixture of chloroform and methanol 2:1 (v/v) [best ratio previously demonstrated (Amato et al. 2019)] and subsequently kept in an ultrasound bath for 10 min. One example of dispersion prepared with this procedure is shown on Fig. SI 1 (Supporting Information), where α-CDs (5 wt%) are observed under daylight and under 365 nm UV light.

After that, the CDs dispersion is added to that of PMMA-chloroform and mixed in an ultrasound bath for 10 min. Different CDs-PMMA systems are prepared according to the desired concentration of CDs, from 0.1 to 5% in mass [for instance, Fig. SI 2 (Supporting Information) shows the aspect of the solution obtained for the system PMMA-NCNDs (5 wt%)].

Next, the optical films are produced by solution casting onto Petri dishes, slowly pouring (drop-by-drop) the CDs-PMMA solution with a pipette. For this step, the dishes are kept at level to evenly maintain the thickness of the casted volume. Finally, the Petri dishes are left to dry in an atmosphere saturated with chloroform vapor (room temperature) for 48–72 h to avoid formation of microvoids due to rapid volatilization. The saturated atmosphere is created by placing several vials containing chloroform close to the Petri dishes, keeping the set covered to ensure isolation from the room. A PMMA casting film with no carbon nanodots (pristine sample) is also prepared through this same procedure. The optical films formed on the Petri dishes are weighed after 24 h, 48 h and 72 h, until the mass losses due to the evaporation of chloroform are stabilized. Figure SI 3 (Supporting Information) shows the aspect and the blue fluorescence observed (λ = 365 nm irradiation) from a PMMA-NCNDs (5 wt%) film formed in the Petri dish. The fluorescence of CDs is stable as long as they are dry and can be dried before use. Once incorporated into the PMMA polymer matrix, the CDs do not suffer from humidity effects and the fluorescence of the optical films remains stable.

Films' fluorescence and photovoltaic characterizations

The PMMA-CDs film is cut with a scalpel from the bottom of the Petri dish in the shape of a 45 mm × 13.5 mm rectangle. Then, the dish is taken to the freezer for 1–2 min to allow the polymeric film to be released from the dish. Thus, the film's mass and thickness are measured before the fluorescence evaluation. Figure 2 shows the aspect of one film formed with PMMA and NCNDs (0.5 wt%) when the material is observed under daylight and under 365 nm-UV light.

PMMA films had their photoluminescence (PL) spectra analyzed at room temperature with a Cary Ellipse-Varian Fluorescence Spectrophotometer (Agilent Technologies) at excitation wavelengths from 300 to 360 nm, 600 nm/min scan speed, and excitation and emission slits of 5 nm. A Fluorolog 3 Fluorescence Spectrophotometer (Horiba)

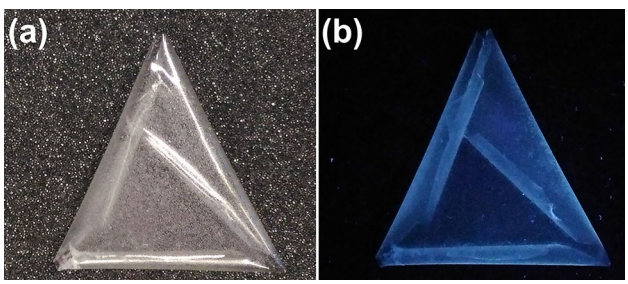

Fig. 2 PMMA-NCNDs films (0.5 wt%) observed under: **a** daylight; **b** UV light (λ = 365 nm)

equipped with sample holders for thin films was used in the characterization of the produced optical films.

Photovoltaic measurements were performed with in-house silicon-based solar cells (laboratory scale, usually destined to didactic purposes) with dimensions of 25 mm × 25 mm and maximum efficiency of 5%. The tests were conducted by positioning and holding the pristine PMMA and doped PMMA-CDs optical films on the surface of the solar cells. The cells were tested on a bench designed for photovoltaic measurements (Stem 2007) equipped with a solar simulator where the light source is a xenon XPS 300 (Solar Light) adjusted for an incident intensity of 1000 W/m^2. A thermostatic bath keeps the cells temperature constant at 25 °C, and the I × V curves of the photovoltaic devices are measured with a digital multimeter HP 34401A (Hewlett Packard) and Lab Tracer 2.0 (Keithley) software. Also, the measurement system uses a standard solar cell with short-circuit current I_{sc} = 66.40 mA for reference purposes. The solar cells and testing bench are shown on Fig. SI 4 (Supporting Information).

Results and discussion

Characterization of films fluorescence emission

The pristine PMMA film exhibits a natural fluorescence emission when irradiated from 300 to 320 nm (broad emission peak around 450 nm), but there is no luminescence for irradiations at longer wavelengths (Fig. 3a). If compared to the pristine material, the PMMA-NCNDs films reveals additional emission bands for excitations longer than 320 nm (Figs. 3b–d). From the films produced using chloroform/methanol 2:1, it is possible to discern the PMMA typical bands without spectral shifts along with the CDs ones with lower intensity. The lower intensity of CDs emissions can

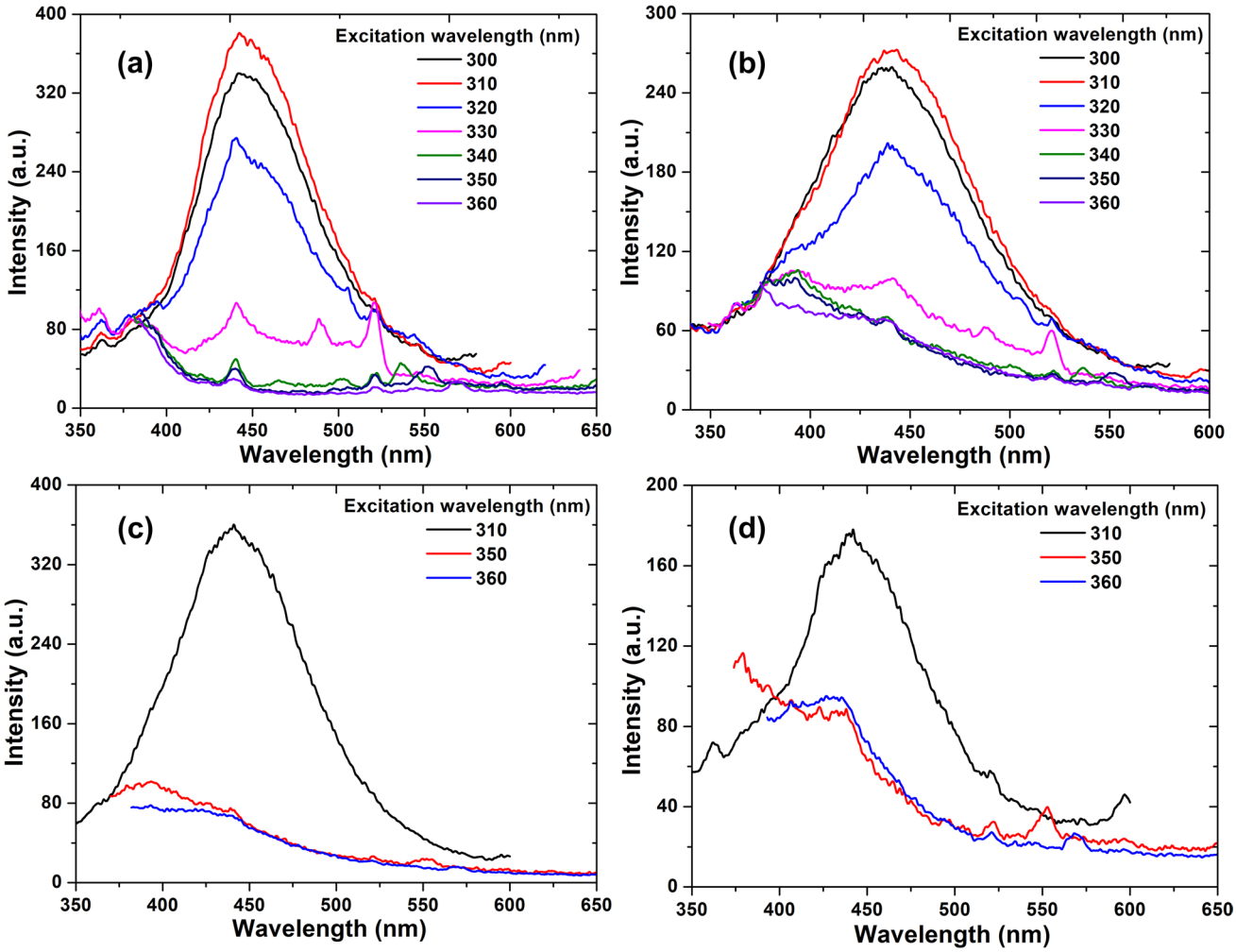

Fig. 3 PL spectra: **a** PMMA pristine film; and different vol. proportions of chloroform to methanol for producing PMMA-NCNDs composites (0.1 wt% of CDs). Proportions of: **b** 2:1 (selected as standard); **c** (3.3):1; **d** 4:1 (v/v)

be explained by several phenomena: (1) low number of light emitters in the matrix (Perli et al. 2022; Gong et al. 2018; Jiang et al. 2020; Lakowicz 2006); (2) low fluorescence quantum yield of the emitters (related to the type of carbon dots used) (Lakowicz 2006); (3) matrix-related effects and the quality of nanoparticles dispersion (modification of the emissive domains on each dot) (Jiang et al. 2020); and (4) solvatochromic effects (Chandra et al. 2019; Bano et al. 2019; Reichardt 2005). In addition, quenching phenomena can occur, as carbon dots can act as electron donors or acceptors in their excited states (Đorđević et al. 2020; Cacioppo et al. 2020). The composition of the solvent mixture (type of CD and its concentration) is a major factor in modulating the fluorescence emission of the film (Fig. 3c, d). This is illustrated by the matrices obtained for chloroform/methanol ratios of 3.3:1 and 4:1 showing PMMA emissions alongside broader NCNDs emission bands with undistinguishable maximum (~400–450 nm). From this data, the solvent mixture ratio 2:1 resulted in the best compromise in terms of NCNDs emission for this study.

To verify the hypotheses that the intensities could be related to the concentration and nature of the occluded carbon nanodots, higher concentrations of NCNDs (5 wt%) were tested and compared against the same concentrations of α-CDs and Silica-Cdots. The PMMA-α-CDs solution used in this study (before casting) is shown on Fig. SI 5 (Supporting Information), whereas the PL results are presented in Fig. 4.

Increasing NCNDs nanoparticles concentration resulted in more well-defined and intense emission bands for the dots emissions, even reaching levels slightly higher than the PMMA matrix. Now, the maxima for emissions from 330 to 360 nm excitations are clearly centered at 450 nm. Thus, the presence of fluorescent nanoparticles extends the range of UV-to-Visible conversion in PMMA up to excitation wavelengths of 360 nm.

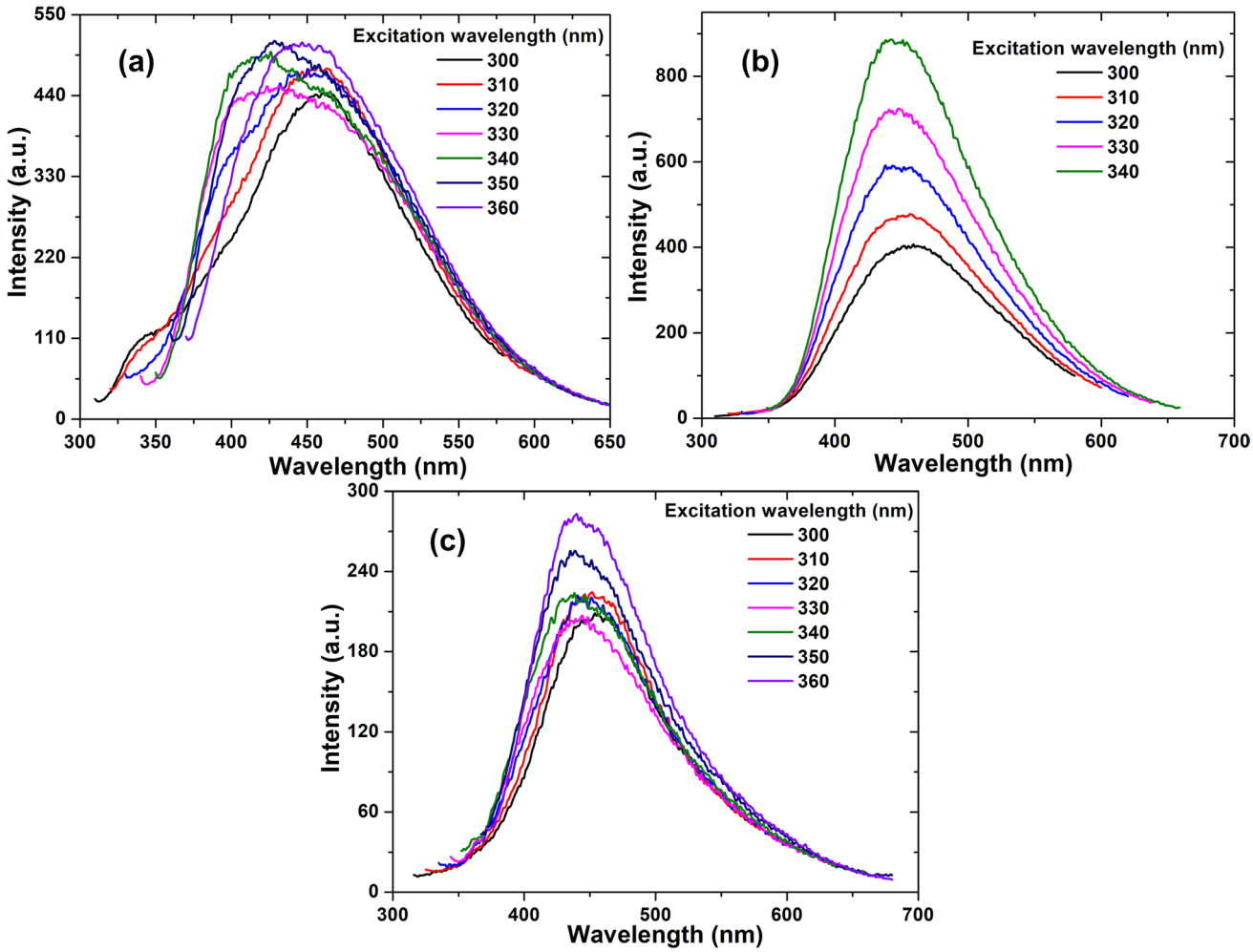

Fig. 4 PL spectra of films produced by doping PMMA with different amounts of nanoparticles (concentration in mass): **a** 5 wt% of NCNDs; **b** 5 wt% of α-CDs (emissions for 350 and 360 nm were omitted, since intensities overcame 1000 a.u. and saturated the detector); and **c** 5 wt% of Silica-Cdots hybrids

Superior spectral energy conversion was obtained when testing α-CDs and Silica-Cdots hybrids in relation to NCNDs, with several emission peaks showing higher intensities than the emissions from the matrix. The peaks are still centered at 450 nm, and Fig. 4b (α-CDs) presents all CDs emissions above the PMMA's (peaks increasing with the excitation wavelength). Emissions observed for 350 and 360 nm excitations overcame 1000 a.u. (arbitrary units) and saturated the detector, so they were omitted from Fig. 4b. Lastly, Fig. 4c shows lower intensities for the hybrids when compared to α-CDs. This is most likely related to the very larger dimensions of the hybrids and to the modification of the surface functional groups originated from the coupling reaction between the α-CDs carboxylic acids and the SiO_2 nanoparticles, which removes some of the free –COOH. Such structural differences modify the interactions between the dispersed phase and the acrylate matrix and can lead to changes in the quenching mechanisms and emissive domains on each nanodot (Amato et al. 2021; Cadranel et al. 2018; Jiang et al. 2020; Bano et al. 2019).

To avoid further detector saturation issues, the previous analysis was repeated, but the excitation and emission slits were reduced from 5 to 2.5 nm. As shown on Figure SI 6 (Supporting Information), the slits reduction results in spectra which much lower intensities: as a matter of fact, only the PMMA-α-CDs system could be analyzed, showing intensities increasing with excitations from 340 to 370 nm and a clear emission maximum at 425 nm, which corresponds to the excitation at 370 nm. This increase of the intensity with the excitation wavelength was not observed on the other systems.

The films observed under daylight and under UV radiation ($\lambda = 365$ nm) are shown in Fig. SI 7 (Supporting Information). Their absorption and transmittance properties, in turn (obtained with the spectrophotometer), are compared in Figs. SI 8–9 (Supporting Information). In Fig. SI 8, the UV–Visible absorption spectra for the nanodots composites show maximum absorbance at 250 nm, corresponding to the $\pi \rightarrow \pi^*$ transition of the sp^2 carbons of the CDs cores. Shoulders at 275–300 nm with tails extending to the visible range are present, assigned to the $n \rightarrow \pi^*$ transitions involving the electron lone pairs of the carboxylic and nitrogen surface groups (Perli et al. 2022; Amato et al. 2021). The pristine sample presents almost no absorbance on the analyzed range, whereas the PMMA-α-CDs is the composite with highest capability of absorbing ultraviolet light. This behavior is approximately opposite to the observed for the transmittances (Fig. SI 9): until 300 nm, pristine has a transmittance considerably higher than the composites, whereas the PMMA-α-CDs shows a slower sigmoidal increase of the transmittance, reaching a value close to 100% only for wavelengths longer than 500 nm. The Silica-Cdots nanocomposite has the highest transmittance on the visible, which may be related to inherent optical properties of silicates (Saleh and Teich 1991; Santos et al. 2011).

Screening of the photovoltaic properties

Carbon nanodots show interesting applications in photocatalysis and renewable energies and can be used in solar concentrators (LSC) or converter (LDS) devices. These devices are designed to collect solar light by absorbing incident photons and reemitting them through an optical waveguide (Wang and Hu 2014; Stepanidenko et al. 2021; Zhao et al. 2022).

In general, the LSC collector is composed of thin plates or sheets of a transparent material doped with luminescent species. Incident sunlight excites these species, and then their reemissions are collected with a waveguide and directed to the photovoltaic cells, improving the energy conversion efficiency (Reisfeld et al. 1988; Barik and Pradhan 2021; Liu et al. 2020). In turn, solar converters (LDS) are films or photoluminescent layers deposited and adhered on the surface of solar cells or photodiodes. LDSs have the same function of shifting the solar spectrum to longer wavelengths (down shifting), converting UV radiation to visible light (Choi et al. 2017; Ahmed et al. 2012).

Due to its great optical properties, PMMA is one of the most applied materials for manufacturing LSCs (Reisfeld et al. 1988) and LDSs (Choi et al. 2017). In general, these LSCs use organic dyes or inorganic quantum dots as fluorescent species, showing disadvantages such as the photodegradation of the organic dyes or the toxicity of the inorganic nanoparticles (Zhou et al. 2015; Waldron et al. 2017; Ahmed et al. 2012). Thus, the photoluminescent behavior of the PMMA-CDs matrices could be exploited to improve the External Quantum Efficiency (EQE) of photovoltaic cells, considering the large-scale systems' production costs (Reisfeld et al. 1988).

Carbon nanodots-based nanocomposites have already been leveraged on solar energy applications (Gong et al. 2018; Li et al. 2017; Choi et al. 2017). In these studies, PMMA-doped films were used as luminescent solar collectors and cells' top-layers, converting UV to visible light. That is because silicon-based solar cells show poor light harvesting performance under UV-irradiation, leading to poor quantum efficiencies in the UV region (Amato et al. 2019; Tsai et al. 2016).

Most of the incident UV photons produce photogenerated carriers (electron–hole pairs) close to the surface, which could easily recombine with defect sites in the depletion region, the intermediary zone of the solar cell's p–n junction where the electric current is generated. In this context, NCNDs could facilitate the down-conversion effect on silicon cells: photons with longer wavelengths (in the visible range) could be absorbed and excite carriers in the depletion

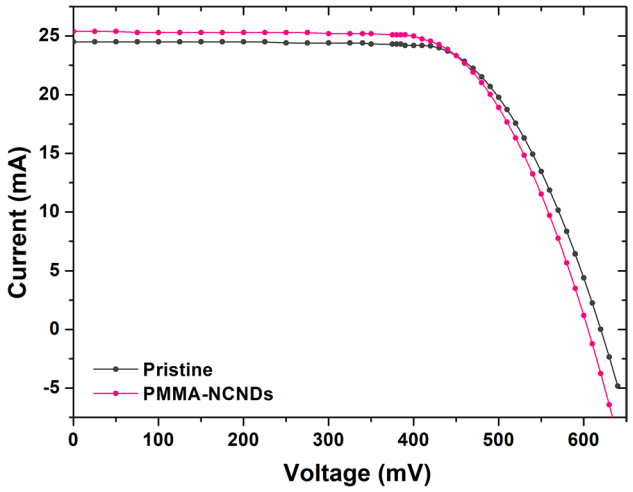

Fig. 5 Curves of current versus voltage for the solar cells with: (blue) pristine sample; and (red) PMMA-NCNDs optical film

Table 1 Photovoltaic data obtained for the two tested solar cells covered with pristine and PMMA-NCNDs optical films

	Pristine	PMMA-NCNDs
I_{sc} (mA)	23.87	26.55
V_{oc} (V)	0.6069	0.6098
J_{sc} (mA/cm^2)	9.95	11.06
P_{max} (mW)	10.18	11.32
FF	0.703	0.699
η (%)	4.24	4.72

region for immediate photogenerated carrier separation due to the built-in electric field, leading to increased photovoltaic effect (Amato et al. 2019; Choi et al. 2017; Tsai et al. 2016).

Therefore, as PMMA-CDs nanocomposites are promising candidates for solar cells applications, NCNDs-doped optical films were used in proof-of-concept experiments on the improvement of cell efficiency by positioning the doped films on the external surfaces of silicon-based solar cells with dimensions of 25 mm × 25 mm.

The photovoltaic results (current I versus voltage V for a given incident irradiance power P_{in}) obtained for the cell with pristine sample are compared to the NCNDs-doped (0.5 wt%) optical film in Fig. 5, and the experimental parameters obtained are shown in Table 1. Here I_{sc} is the short-circuit current, which is the maximum current that may occur on the cell (zero-voltage condition). This current is due to the generation and collection of light-generated carriers and, for an ideal solar cell at moderate resistive loss mechanisms, it is identical to the light-generated current (Honsberg and Bowden 2019a). The open-circuit voltage V_{oc}, in turns, is the maximum voltage available for a solar cell, occurring at zero current. It corresponds to the amount of forward bias on the solar cell due to the bias of the cell junction with the light-generated current (Honsberg and Bowden 2019b).

V_{oc} presents a complex non-linear relation with temperature and increases with the bandgap, whereas I_{sc} decreases with this gap. In an ideal device, V_{oc} is limited by radiative recombination (electron–hole) (Honsberg and Bowden 2019b). I_{sc}, on the other hand, depends on a series of factors, including: (1) the area of the solar cell; (2) the number of incident photons, or power of the incident light source P_{in}; (3) the spectrum of the incident light; (4) the optical properties (absorption, transmittance and reflection) of the solar cell; and (5) the minority-carrier collection probability of the solar cell, which mainly depends on the surface passivation and on the minority carrier lifetime in the cell's base (Honsberg and Bowden 2019a). For both I_{sc} and V_{oc} conditions, the power produced by the cell is zero. So, the fill factor (FF) is a parameter used in conjunction with I_{sc} and V_{oc} to determine the efficiency of the cell. It is given by the relation between the maximum power P_{max} of the cell and the product between I_{sc} and V_{oc}. This relation is defined as Eq. (1) (Honsberg and Bowden 2019c).

$$FF = \frac{P_{max}}{\left(V_{OC} \times I_{SC}\right)} \tag{1}$$

FF may be understood as a measurement of the "*squareness*" of the solar cell's I × V curve and is also the area of the largest rectangle which may be inscribed in this plot. The FF from a solar cell can be determined by differentiating its power with respect to the voltage and finding the maximum P_{max} (dP/dV = 0): the rectangle area is obtained by multiplying the V of maximum power by the correspondent current value retrieved from I curve (Honsberg and Bowden 2019c). From these parameters, the efficiency of the solar cell η may be finally calculated as Eq. (2) or, in percentage, as Eq. (3) (Gong et al. 2018).

$$\eta = \frac{\left(J_{SC} \times V_{OC} \times FF\right)}{P_{in}} \tag{2}$$

$$\eta = \frac{\left(J_{SC} \times V_{OC} \times FF\right)}{P_{in}} \times 100\% \tag{3}$$

The current density J_{sc} is related to the cell's transmission and to the amount of excited photoelectrons in the device, presenting a great influence on the overall efficiency of the system (Chung et al. 2012). Moreover, previous studies with carbon nanodots-doped light solar concentrators indicate that both J_{sc} and V_{oc} should increase with the concentration of nanoparticles. Since the total of excited photoelectrons is associated with the doping concentration, the intensity of the emitted fluorescence increases with CDs concentration. Gong et al. (2018) argue that such increase is not indefinite, though,

so the concentration of nanoparticles has an optimal value. This comes from overlaps between the absorption spectra and the fluorescence emission spectra of carbon nanodots leading to reabsorption of emitted photons by the CDs themselves. Finally, as the fluorescence quantum efficiency must be smaller than 1 (Lakowicz 2006), the final emitted fluorescence intensity is necessarily smaller than the absorbed intensity, resulting in a loss of energy in the conversion process. Therefore, if the doping concentration exceeds the optimum value (a condition that must be determined empirically), the fluorescence intensity and the solar cell's efficiency will start decreasing (Gong et al. 2018).

In Fig. 5 and Table 1, the I×V curve and photovoltaic parameters are presented for a PMMA-0.5 wt% NCNDs and pristine optical films of ~ 35 μm thicknesses. An increase in the solar cell efficiency is observed for the NCNDs-doped matrix, from 4.24 to 4.72%. Even though at first glance this 11.3% increase might seem of low significance, it can be translated into substantial savings of economic and environmental resources on commercial systems. For instance, a typical panel has an efficiency of 15% and surface area of 1 m^2, producing about 150 W of electrical energy (Vourvoulias 2023). Employing such panels, the National Renewable Energy Laboratory (NREL—USA) estimates that 2.8 acres of panels are needed to supply 1000 households with electricity for a year (1 GWh), corresponding to 32 acres of land for the solar farm (Business 2013; Ong et al. 2013). Thus, an efficiency increase of 11.3% would bring the net panel efficiency up to 16.7%, reducing the total area of the panels to 2.5 acres (10.7% reduction); and lowering the total land needed for the solar plant to 28.7 acres (10.3% reduction).

Furthermore, the current experimental setup is based on the simple partial superposition of the optical films on the cell's surfaces, leading to limiting factors to the efficiency gain such as poor interface contact conditions and the possible formation of an intermediate air layer (dielectric). Light reflections may be observed on a setup like this, as the PMMA layer is not adhered on the cell surface and the film thickness was not optimized for interferometric anti-reflexive properties. Spurious reflections reduce the conversion efficiency by partially rejecting light back to the external medium. Therefore, the reduction of the film's reflectance could be a strategy for improving the energy conversion (Saleh and Teich 1991; Taylor 2002). Naturally, the use of the most-efficient carbon nanodots (α-CDs) is also expected to lead to better results, since they present the most intense emissions.

Conclusions

Three typologies of carbon dots, namely NCNDs, α-CDs and Silica-Cdots hybrids, were applied to the fabrication of fluorescent PMMA optical films, significantly enhancing the PMMA's natural fluorescence and allowing the conversion of a wider UV wavelength spectrum to visible for increased solar cell efficiency. Initial testing showed an 11.3% increase in efficiency by employing fluorescent films, even in not optimized conditions. This gain is translated in up to 10.3% of land use reduction in solar plants functionalized with fluorescent films to generate the same amount of power as regular panels, showing the feasibility and potential application of these low-cost sustainable materials.

Upcoming works will focus on optimizing the usage of α-CDs (that present the highest UV-to-Visible conversion) as the standard for fluorescent film fabrication, to further enhance efficiency gains. Since these nanoparticles are formed by thermolysis in simple muffles, they are particularly adequate for large-scale manufacturing due to requiring simpler, cheaper and easily scalable equipment. In addition to larger efficiency gains, as very high UV absorbance is observed for α-CDs (Fig. SI 8), doped PMMA films will help protect the cell against UV-induced degradation to the passivation layers, increasing the lifespan of panels and leading to reduced maintenance costs. Methodologies for direct coating of the cells with doped films will also be investigated to eliminate the extra dielectric layer (air gaps) and minimize reflection losses. Potential avenues to accomplish this are drop-casting the PMMA-CDs chloroform solutions directly on the cell's surface, and spin-coating.

Supplementary Information The online version contains supplementary material available at https://doi.org/10.1007/s43153-023-00408-w.

Acknowledgements Authors thank São Paulo Research Foundation (FAPESP) for the financial support (Grants 2019/22554-4 and 2018/08782-1); Coordenação de Aperfeiçoamento de Pessoal de Nivel Superior–Brazil (CAPES), finance code 001; National Council for Scientific and Technological Development (CNPq), finance code 001; M.P. is the AXA Chair for Bionanotechnology (2016-2023). This study was supported by the University of Trieste, INSTM; the Italian Ministry of Education, MIUR (cofin Prot. 2017PBXPN4); and the Spanish Ministry of Science, Innovation and Universities, MICIU (project PID2019-108523RB-I00). Part of this research was performed under the Maria de Maeztu Units of Excellence Program from the Spanish State Research Agency, Grant no. MDM-2017-0720. We also thank Prof. Maurizio Prato, Dr. Francesca Arcudi, Dr. Giacomo Filippini and Beatrice Bartolomei from the Carbon Nanotechnology Group, Department of Chemical and Pharmaceutical Sciences, University of Trieste (Italy); and Igor Abbe from the Laboratory of Microelectronics, Polytechnic School, University of São Paulo, SP, Brazil for the technical and experimental support and insights on data interpretation.

Data availability Data of this research is available upon request to the correspondent authors.

Declarations

Conflict of interest On behalf of all authors, the corresponding author states that there is no conflict of interest.

References

Affonso Netto R, de Menezes FF, Maciel Filho R, Bartoli JR (2022) Poly(methyl methacrylate) and silica nanocomposites as new materials for polymeric optical devices. Polímeros. https://doi.org/10.1590/0104-1428.20220009

Ahmed H, Kennedy M, Confrey T, Doran J, McCormack SJ, Galindo S, Sánchez CV, González JP (2012) Lumogen violet dye as luminescent down-shifting layer for c-silicon solar cells. In: 27th European photovoltaic solar energy conference and exhibition, Frankfurt, Germany, 24–28 September 2012, pp 311–313. https://doi.org/10.4229/27thEUPVSEC2012-1BV.7.20

Albaladejo-Siguan M, Baird EC, Becker-Koch D, Li Y, Rogach AL, Vaynzof Y (2021) Stability of quantum dot solar cells: a matter of (life)time. Adv Energy Mater 11:2003457. https://doi.org/10.1002/aenm.202003457

Alexandre M, Dubois P (2000) Polymer-layered silicate nanocomposites: preparation, properties and uses of a new class of materials. Mater Sci Eng R Rep 28:1–63. https://doi.org/10.1016/S0927-796X(00)00012-7

Ali U, Karim KJBA, Buang NA (2015) A review of the properties and applications of poly (methyl methacrylate) (PMMA). Polym Rev 55:678–705. https://doi.org/10.1080/15583724.2015.1031377

Amato F, Cacioppo M, Arcudi F, Prato M, Mituo M, Fernandes EG, Carreño MNP, Pereyra I, Bartoli JR (2019) Nitrogen-doped carbon nanodots/PMMA nanocomposites for solar cells applications. Chem Eng Trans 74:1105–1110. https://doi.org/10.3303/CET1974185

Amato F, Soares MCP, Cabral TD, Fujiwara E, Cordeiro CMB, Criado A, Prato M, Bartoli JR (2021) Agarose-based fluorescent waveguide with embedded silica nanoparticle-carbon nanodot hybrids for pH sensing. ACS Appl Nano Mater 4:9738–9751. https://doi.org/10.1021/acsanm.1c02127

Arcudi F, Đorđević L, Prato M (2016) Synthesis, separation, and characterization of small and highly fluorescent nitrogen-doped carbon nanoDots. Angew Chem Int Ed 55:2107–2112. https://doi.org/10.1002/ange.201510158

Arcudi F, Đorđević L, Prato M (2017) Rationally designed carbon nanodots towards pure white-light emission. Angew Chem Int Ed 56:4170–4173. https://doi.org/10.1002/anie.201612160

Bano D, Kumar V, Singh VK, Chandra S, Singh DK, Yadav PK, Talat M, Hasan SH (2019) A facile and simple strategy for the synthesis of label free carbon quantum dots from the latex of *Euphorbia milii* and its peroxidase-mimic activity for the naked eye detection of glutathione in a human blood serum. ACS Sustain Chem Eng 7:1923–1932. https://doi.org/10.1021/acssuschemeng.8b04067

Barik P, Pradhan M (2021) Plasmonic luminescent solar concentrator. Sol Energy 216:61–74. https://doi.org/10.1016/j.solener.2021.01.018

Bartolomei B, Dosso J, Prato M (2021) New trends in nonconventional carbon dot synthesis. Trends Chem 3:943–953. https://doi.org/10.1016/j.trechm.2021.09.003

Boakye-Yiadom KO, Kesse S, Opoku-Damoah Y, Filli MS, Aquib M, Joelle MMB, Farooq MA, Mavlyanova R, Raza F, Bavi R, Wang B (2019) Carbon dots: applications in bioimaging and theranostics. Int J Pharm 564:308–317. https://doi.org/10.1016/j.ijpharm.2019.04.055

Bottrill M, Green M (2011) Some aspects of quantum dot toxicity. Chem Commun 47:7039. https://doi.org/10.1039/c1cc10692a

Bouknaitir I, Panniello A, Teixeira SS, Kreit L, Corricelli M, Striccoli M, Costa LC, Achour ME (2019) Optical and dielectric properties of PMMA (poly(methyl methacrylate))/carbon dots composites. Polym Compos 40:E1312–E1319. https://doi.org/10.1002/pc.24977

Bressanin JM, Júnior VA, Bartoli JR (2018) Electrically conductive nanocomposites of PMMA and carbon nanotubes prepared by in situ polymerization under probe sonication. Chem Pap 72:1799–1810. https://doi.org/10.1007/s11696-018-0443-5

Business S (2013) How much land does it take to produce solar energy for 1000 Homes? https://www.sustainablebusiness.com/2013/08/how-much-land-does-it-take-to-produce-solar-energy-for-1000-homes-51784/. Accessed 12 Mar 2023

Cacioppo M, Scharl T, Đorđević L, Cadranel A, Arcudi F, Guldi DM, Prato M (2020) Symmetry-breaking charge-transfer chromophore interactions supported by carbon nanodots. Angew Chem Int Ed 59:12779–12784. https://doi.org/10.1002/anie.202004638

Cadranel A, Strauss V, Margraf JT, Winterfeld KA, Vogl C, Đorđević L, Arcudi F, Hoelzel H, Jux N, Prato M, Guldi DM (2018) Screening supramolecular interactions between carbon nanodots and porphyrins. J Am Chem Soc 140:904–907. https://doi.org/10.1021/jacs.7b12434

Chandra S, Singh VK, Yadav PK, Bano D, Kumar V, Pandey VK, Talat M, Hasan SH (2019) Mustard seeds derived fluorescent carbon quantum dots and their peroxidase-like activity for colorimetric detection of H_2O_2 and ascorbic acid in a real sample. Anal Chim Acta 1054:145–156. https://doi.org/10.1016/j.aca.2018.12.024

Choi Y, Jo S, Chae A, Kim YK, Park JE, Lim D, Park SY, In I (2017) Simple microwave-assisted synthesis of amphiphilic carbon quantum dots from A 3 /B 2 polyamidation monomer set. ACS Appl Mater Interfaces 9:27883–27893. https://doi.org/10.1021/acsami.7b06066

Chung I, Lee B, He J, Chang RPH, Kanatzidis MG (2012) All-solid-state dye-sensitized solar cells with high efficiency. Nature 485:486–489. https://doi.org/10.1038/nature11067

Corsaro C, Neri G, Santoro A, Fazio E (2021) Acrylate and methacrylate polymers' applications: second life with inexpensive and sustainable recycling approaches. Materials (basel) 15:282. https://doi.org/10.3390/ma15010282

Đorđević L, Arcudi F, Prato M (2019) Preparation, functionalization and characterization of engineered carbon nanodots. Nat Protoc 14:2931–2953. https://doi.org/10.1038/s41596-019-0207-x

Đorđević L, Haines P, Cacioppo M, Arcudi F, Scharl T, Cadranel A, Guldi DM, Prato M (2020) Synthesis and excited state processes of arrays containing amine-rich carbon dots and unsymmetrical rylene diimides. Mater Chem Front 4:3640–3648. https://doi.org/10.1039/D0QM00407C

Đorđević L, Arcudi F, Cacioppo M, Prato M (2022) A multifunctional chemical toolbox to engineer carbon dots for biomedical and energy applications. Nat Nanotechnol 17:112–130. https://doi.org/10.1038/s41565-021-01051-7

Fischer H (2003) Polymer nanocomposites: from fundamental research to specific applications. Mater Sci Eng C 23:763–772. https://doi.org/10.1016/j.msec.2003.09.148

Ghosh T, Das TK, Das P, Banerji P, Das NC (2022) Current scenario and recent advancement of doped carbon dots: a short review scientocracy update (2013–2022). Carbon Lett 32:953–977. https://doi.org/10.1007/s42823-022-00339-5

Gong X, Ma W, Li Y, Zhong L, Li W, Zhao X (2018) Fabrication of high-performance luminescent solar concentrators using N-doped carbon dots/PMMA mixed matrix slab. Org Electron 63:237–243. https://doi.org/10.1016/j.orgel.2018.09.028

Gong X, Zheng S, Zhao X, Vomiero A (2022) Engineering high-emissive silicon-doped carbon nanodots towards efficient large-area luminescent solar concentrators. Nano Energy 101:107617. https://doi.org/10.1016/j.nanoen.2022.107617

Honsberg CB, Bowden SG (2019a) Short-circuit current. Photovoltaics Educ. Website. https://www.pveducation.org/pvcdrom/solar-cell-operation/short-circuit-current. Accessed 24 Jan 2023

Honsberg CB, Bowden SG (2019b) Open-circuit voltage. Photovoltaics Educ. https://www.pveducation.org/pvcdrom/solar-cell-operation/open-circuit-voltage. Accessed 24 Jan 2023

Honsberg CB, Bowden SG (2019c) Fill factor. Photovoltaics Educ. https://www.pveducation.org/pvcdrom/solar-cell-operation/fill-factor. Accessed 24 Jan 2023

Huang X, Zhang F, Zhu L, Choi KY, Guo N, Guo J, Tackett K, Anilkumar P, Liu G, Quan Q, Choi HS, Niu G, Sun Y-P, Lee S, Chen X (2013) Effect of injection routes on the biodistribution, clearance, and tumor uptake of carbon dots. ACS Nano 7:5684–5693. https://doi.org/10.1021/nn401911k

Huang K, Liu J, Yuan J, Zhao W, Zhao K, Zhou Z (2023) Perovskite-quantum dot hybrid solar cells: a multi-win strategy for high performance and stability. J Mater Chem A 11:4487–4509. https://doi.org/10.1039/D2TA09434G

Jiang K, Wang Y, Li Z, Lin H (2020) Afterglow of carbon dots: mechanism, strategy and applications. Mater Chem Front 4:386–399. https://doi.org/10.1039/C9QM00578A

Kang Z, Lee S-T (2019) Carbon dots: advances in nanocarbon applications. Nanoscale 11:19214–19224. https://doi.org/10.1039/C9NR05647E

Kwon W, Do S, Lee J, Hwang S, Kim JK, Rhee S-W (2013) Freestanding luminescent films of nitrogen-rich carbon nanodots toward large-scale phosphor-based white-light-emitting devices. Chem Mater 25:1893–1899. https://doi.org/10.1021/cm400517g

Lakowicz JR (2006) Principles of fluorescence spectroscopy, 3rd edn. Springer US, Boston. https://doi.org/10.1007/978-0-387-46312-4

Li Y, Miao P, Zhou W, Gong X, Zhao X (2017) N-doped carbon-dots for luminescent solar concentrators. J Mater Chem a 5:21452–21459. https://doi.org/10.1039/C7TA05220K

Li J, Zhao H, Zhao X, Gong X (2023) Boosting efficiency of luminescent solar concentrators using ultra-bright carbon dots with large Stokes shift. Nanoscale Horizons 8:83–94. https://doi.org/10.1039/D2NH00360K

Lin X, Yang Y, Nian L, Su H, Ou J, Yuan Z, Xie F, Hong W, Yu D, Zhang M, Ma Y, Chen X (2016) Interfacial modification layers based on carbon dots for efficient inverted polymer solar cells exceeding 10% power conversion efficiency. Nano Energy 26:216–223. https://doi.org/10.1016/j.nanoen.2016.05.011

Liu G, Mazzaro R, Sun C, Zhang Y, Wang Y, Zhao H, Han G, Vomiero A (2020) Role of refractive index in highly efficient laminated luminescent solar concentrators. Nano Energy 70:104470. https://doi.org/10.1016/j.nanoen.2020.104470

Ma W, Li W, Liu R, Cao M, Zhao X, Gong X (2019) Carbon dots and AIE molecules for highly efficient tandem luminescent solar concentrators. Chem Commun 55:7486–7489. https://doi.org/10.1039/C9CC02676B

Manshian BB, Jiménez J, Himmelreich U, Soenen SJ (2017) Personalized medicine and follow-up of therapeutic delivery through exploitation of quantum dot toxicity. Biomaterials 127:1–12. https://doi.org/10.1016/j.biomaterials.2017.02.039

Maxim AA, Sadyk SN, Aidarkhanov D, Surya C, Ng A, Hwang Y-H, Atabaev TS, Jumabekov AN (2020) PMMA thin film with embedded carbon quantum dots for post-fabrication improvement of light harvesting in perovskite solar cells. Nanomaterials 10:291. https://doi.org/10.3390/nano10020291

Mazzucco ML, Marchesin MS, Fernandes EG, Da Costa RA, Marini J, Bretas RE, Bartoli JR (2016) Nanocomposites of acrylonitrile-butadiene-styrene/montmorillonite/styrene block copolymers: structural, rheological, mechanical and flammability studies on the effect of organoclays and compatibilizers using statistically designed experiments. J Compos Mater 50:771–782. https://doi.org/10.1177/0021998315581509

Mohan K, Bora A, Dolui SK (2018) Efficient way of enhancing the efficiency of a quasi-solid-state dye-sensitized solar cell by harvesting the unused higher energy visible light using carbon Dots. ACS Sustain Chem Eng 6:10914–10922. https://doi.org/10.1021/acssuschemeng.8b02244

Moon H, Lee C, Lee W, Kim J, Chae H (2019) Stability of quantum dots, quantum dot films, and quantum dot light-emitting diodes for display applications. Adv Mater 31:1804294. https://doi.org/10.1002/adma.201804294

Ong S, Campbell C, Denholm P, Margolis R, Heath G (2013) Land-use requirements for solar power plants in the United States. https://www.nrel.gov/docs/fy13osti/56290.pdf. Accessed 24 Jan 2023

Perli G, Soares MCP, Cabral TD, Bertuzzi DL, Bartoli JR, Livi S, Duchet-Rumeau J, Cordeiro CMB, Fujiwara E, Ornelas C (2022) Synthesis of carbon nanodots from sugarcane syrup, and their incorporation into a hydrogel-based composite to fabricate innovative fluorescent microstructured polymer optical fibers. Gels 8:553. https://doi.org/10.3390/gels8090553

Prado BR, Bartoli JR (2018) Synthesis and characterization of PMMA and organic modified montmorilonites nanocomposites via in situ polymerization assisted by sonication. Appl Clay Sci 160:132–143. https://doi.org/10.1016/j.clay.2018.02.035

Reichardt C (2005) Polarity of ionic liquids determined empirically by means of solvatochromic pyridinium N-phenolate betaine dyes. Green Chem 7:339–351. https://doi.org/10.1039/b500106b

Reisfeld R, Eyal M, Chernyak V, Zusman R (1988) Luminescent solar concentrators based on thin films of polymethylmethacrylate on a polymethylmethacrylate support. Sol Energy Mater 17:439–455. https://doi.org/10.1016/0165-1633(88)90004-4

Remanan S, Ghosh S, Das TK, Sharma M, Bose M, Bose S, Das AK, Das NC (2020) Gradient crystallinity and its influence on the poly(vinylidene fluoride)/poly(methyl methacrylate) membrane-derived by immersion precipitation method. J Appl Polym Sci. https://doi.org/10.1002/app.48677

Saleh BEA, Teich MC (1991) Fundamentals of photonics. Wiley, New York. https://doi.org/10.1002/0471213748

Santos JS, Ono E, Fujiwara E, Manfrim TP, Suzuki CK (2011) Control of optical properties of silica glass synthesized by VAD method for photonic components. Opt Mater (amst) 33:1879–1883. https://doi.org/10.1016/j.optmat.2011.03.007

Soares M, Amato F, Cabral T, Cacioppo M, Carreño M, Pereyra I, Ramos C, Cid M, Goveia G, Chubaci J, Prato M, Bartoli J, Fujiwara E (2023) Improving solar cells efficiency with PMMA-carbon dots nanocomposites. In: 2023 International Conference optical MEMS Nanophotonics Sbfot. Int. Opt. Photonics Conf. (Sbfot. IOPC). IEEE, pp 1–2. https://doi.org/10.1109/OMN/SBFotonIOPC58971.2023.10230988

Stem N (2007) Células solares de silício de alto rendimento: otimizações teóricas e implementações experimentais utilizando processos de baixo custo. Universidade de São Paulo, São Paulo. https://doi.org/10.11606/T.3.2007.tde-02042008-113959

Stepanidenko EA, Ushakova EV, Fedorov AV, Rogach AL (2021) Applications of carbon dots in optoelectronics. Nanomaterials 11:364. https://doi.org/10.3390/nano11020364

Taylor HF (2002) Fiber optic sensors based upon the fabry-perot interferometer. In: Yu FTS, Yin S (eds) Fiber optic sensors. Marcel Dekker, New York

Tsai M-L, Tu W-C, Tang L, Wei T-C, Wei W-R, Lau SP, Chen L-J, He J-H (2016) Efficiency enhancement of silicon heterojunction solar cells via photon management using graphene quantum dot as downconverters. Nano Lett 16:309–313. https://doi.org/10.1021/acs.nanolett.5b03814

Tuerhong M, Xu Y, Yin X-B (2017) Review on carbon dots and their applications. Chin J Anal Chem 45:139–150. https://doi.org/10.1016/S1872-2040(16)60990-8

Vourvoulias A (2023) Solar panels. GreenMatch. https://www.greenmatch.co.uk/blog/2014/11/how-efficient-are-solar-panels. Accessed 12 Mar 2023

Waldron DL, Preske A, Zawodny JM, Krauss TD, Gupta MC (2017) PbSe quantum dot based luminescent solar concentrators. Nanotechnology 28:095205. https://doi.org/10.1088/1361-6528/aa577f

Wang Y, Hu A (2014) Carbon quantum dots: synthesis, properties and applications. J Mater Chem C 2:6921. https://doi.org/10.1039/C4TC00988F

Wang B, Lu S (2022) The light of carbon dots: from mechanism to applications. Matter 5:110–149. https://doi.org/10.1016/j.matt.2021.10.016

Wu T, Tang M (2014) Toxicity of quantum dots on respiratory system. Inhal Toxicol 26:128–139. https://doi.org/10.3109/08958378.2013.871762

Xia C, Zhu S, Feng T, Yang M, Yang B (2019) Evolution and synthesis of carbon dots: from carbon dots to carbonized polymer dots. Adv Sci 6:1901316. https://doi.org/10.1002/advs.201901316

Yan F, Li J, Zhao X, Gong X (2023) Unveiling unconventional luminescence behavior of multicolor carbon dots derived from phenylenediamine. J Phys Chem Lett 14:5975–5984. https://doi.org/10.1021/acs.jpclett.3c01497

Zhao H (2019) Refractive index dependent optical property of carbon dots integrated luminescent solar concentrators. J Lumin 211:150–156. https://doi.org/10.1016/j.jlumin.2019.03.039

Zhao W-S, Li X-X, Zha H, Yang Y-Z, Yan L-P, Luo Q, Liu X-G, Wang H, Ma C-Q, Xu B-S (2022) Controllable photoelectric properties of carbon dots and their application in organic solar cells. Chin J Polym Sci 40:7–20. https://doi.org/10.1007/s10118-021-2637-5

Zhou W, Wang M-C, Zhao X (2015) Poly(methyl methacrylate) (PMMA) doped with DCJTB for luminescent solar concentrator applications. Sol Energy 115:569–576. https://doi.org/10.1016/j.solener.2015.03.012